RSC Advances

PAPER

View Article Online
View Journal | View Issue

Cite this: *RSC Adv.*, 2020, **10**, 11743

Ionic self-assembled organogel polyelectrolytes for energy storage applications†

José A. Ávila-Niño *[a] and Lilian I. Olvera*[ab]

High performance organogel polyelectrolytes were synthesized by super acid catalyst step-growth polycondensation of isatin and the non-activated multiring aromatic *p*-terphenyl. Subsequently, a chemical modification reaction was carried out to obtained quaternary ammonium functionalized polyelectrolytes through a nucleophilic substitution reaction with (3-bromopropyl)trimethylammonium bromide and potassium carbonate at room temperature. Different functionalization degrees were obtained by controlling the molar ratio of the polymer and the modification agent. The organogel polyelectrolytes were formed due to the high phase segregation and self-assembling observed owing to the amphiphilic character of the material (hydrophobic backbone and hydrophilic fragment grafted). The organogel polyelectrolytes were used to fabricate supercapacitors using two commercial graphite electrodes. These polyelectrolytes displayed good ionic conductivity without the use of another doping agent such as salts, acids or ionic liquids. In this work, a strong correlation of functionalization degree and ionic conductivity of the polyelectrolytes and capacitance of the supercapacitors was observed. The ionic conductivity of the polyelectrolytes reached 0.46 mS cm^{-1} for the 100% functionalization degree, meanwhile the polyelectrolyte with the 10% functionalization degree shows 0.036 mS cm^{-1}. Li-doped polyelectrolytes showed higher ionic conductivity due the presence of extra ionic charges (2.26 and 0.2 mS cm^{-1} for the polyelectrolytes with the 100% and 10% of functionalization degree, respectively). The principal novelty of this work lies in the possibility of modulating the ionic conductivity of organogels and the capacitance of supercapacitors by chemical modifications. The capacitance of the supercapacitors was 1.17 mF cm^{-2} for the 100% functionalized polyelectrolyte and is higher in comparison with the polyelectrolyte with 10% functionalization degree (0.68 mF cm^{-2}) measured at a discharge current of 52 μA cm^{-2} by galvanostatic charge discharge technique. Additionally, when lithium salt (lithium triflate) was added, the polyelectrolytes retained a gel consistency, increasing the ionic conductivity and capacitance. For the doped polyelectrolytes, the areal capacitance reaches 1.37 mF cm^{-2} for the 100% functionalization degree polyelectrolyte with lithium triflate. These organogel polyelectrolytes open the possibility to design flexible and all solid-state supercapacitors without the risk of leakage.

Received 28th January 2020
Accepted 14th March 2020

DOI: 10.1039/d0ra00825g

rsc.li/rsc-advances

Introduction

The increase in the demand for the storage of electrical energy requires the manufacturing of planar and flexible devices for wearable and portable electronics.[1–3] Supercapacitors (SC) are an emerging class of energy storage devices[4] that exhibit more capacitance and energy density than conventional capacitors and are very attractive for portable electronics and automotive applications due to the delivery of a high power density compared to batteries.[5] The electrical double layer capacitors (EDLC)[6] is a type of SC that uses carbon materials as electrodes with high porosity and large surface area. In these capacitors, the double layer formation between ions in an electrolyte and the porous structure of the carbon electrodes is responsible for the high capacitance.[7] In this type of SCs, the energy is stored only by electrostatic processes by adsorption of ions in the interface without faradaic reactions.[8]

The next generation of portable electronics will demand flexible and safe energy storage devices. One of the main problems that hinder the fabrication of flexible SCs is the use of liquid electrolytes which makes the device heavier and prone to leakages. In addition, the device must be encapsulated, which generates an increase of costs[9] and most of the liquid electrolytes are toxic and harmful.[2]

[a]*CONACYT – Center of Research and Technological Development in Electrochemistry (CIDETEQ), Parque Tecnológico Querétaro, Sanfandila, Pedro Escobedo, Querétaro, C. P. 76703, Mexico. E-mail: javila@cideteq.mx; lolvera@materiales.unam.mx*

[b]*Instituto de Investigaciones en Materiales, Universidad Nacional Autónoma de México, Apartado Postal 70-360, CU, Coyoacán 04510, México D. F., Mexico*

† Electronic supplementary information (ESI) available. See DOI: 10.1039/d0ra00825g

The ability of a solution to self-organize has emerged as a great approach to access a large number of structures and architectures, especially networks or gel-like arrangements with unique properties and commercial applications. The gel polymers show considerable conductivities and good mechanical properties and play multiple roles in SC, for instance as electrolytes, binders and separators.[10,11] Generally, in SCs, the gel polymer electrolytes consist of a polymer network or a three-dimensional molecular arrangement, which is used as a host material, mixed with ionic liquids or conducting salts, that are the responsible elements of the ionic conduction.[1,12]

The three dimensional molecular arrangement or a supramolecular structure, due to the ability of a solution to self-organized has emerged as a great approach to access a large number of structures and especially networks or gel-like arrangements.[13] The generation of these types of structures will depend mainly on the substances involved, the chemical functionality and the strength and directionality of the secondary interactions present in the different systems. In supramolecular chemistry, these interactions are mainly hydrogen bondings, amphiphilic, van der Waals forces and ionic.[14]

In polyelectrolytes also depends on the polyelectrolytic chain arrangement, the counterions present and their distribution throughout the polyelectrolyte. Self-assembling processes involve electrostatic interactions between the polyelectrolyte, counterions and solvent and it has been observed that different counterions can induce a non-covalent cross-linking of the polyelectrolyte chains in a network arrangement.[15–17]

Most of the gel polymer electrolytes reported are composed of polyvinyl alcohol (PVA) mixed mainly with H_2SO_4, KOH or LiCl[18–20] but other host polymers such as polymethylmethacrylate (PMMA), poly(vinylidene fluoride-*co*-hexafluoropropylene) (PVdF-HFP), polyacrylonitrile (PAN) or poly(ethylene oxide) PEO have been also employed.[7]

In this work, a cationic polymer was used as organogel polyelectrolyte and separator for energy storage applications using two commercial graphite bars as electrodes. Different percentages of charged units in the organogel polyelectrolytes (functionalization degree) were studied by cyclic voltammetry, galvanostatic charge discharge (GCD) and electrochemical impedance spectroscopy (EIS), showing that ionic conductive and capacitance increased with the functionalization degree increment. This implies that the capacitance of the SCs can be controlled by chemical reactions. Additionally, lithium triflate (LiTf) salt was added to the organogel polyelectrolyte to improve the performance of the SCs and their electrochemical properties, decreasing the resistance. The SCs using gel polyelectrolytes were characterized by a two electrodes configuration to obtain the areal and gravimetric capacitance of the SCs.

Experimental

Polymer synthesis

The synthesis was carried out using a precursor polymer obtained by polycondensation of isatin with the nonactivated, multiring aromatic, *para*-terphenyl (PNH). The reaction was carried out in the Brønsted superacid trifluoromethanesulfonic acid or in a mixture with dichloromethane. Subsequently, a chemical modification reaction was carried out to obtain polymers with positive charges (quaternary ammonium groups, QA) in the main chain (PNQAX, X = functionalization degree). Thus the typical modification of the polymer precursor to obtained polyelectrolyte type gel is described as follows, in a single-necked flask equipment with a magnetic stirred, the polymer precursor was dissolved in NMP 10% w/v once the complete dissolution of the polymer was achieved different amounts of the base K_2CO_3 and the modification reagent were added to obtain the polyelectrolytes with different functionalization degrees. The reaction mixture was stirred for 24 h at room temperature.

Gel polyelectrolyte self assembling

The gel polyelectrolytes were obtained by dissolving cationic polymer fibers in DMSO 10% w/v and after a period of time the self-assembling took place to obtain the gel type polyelectrolytes. Additional samples were obtained with the addition of lithium triflate in a 0.3 M concentration respect to the polymer solution.

Cell fabrication and analysis

Commercial graphite bars were used as electrodes without the use of any current collector. The gel type polymer was used as electrolyte and separator and was placed in the middle of the two graphite bars. The cyclic voltammetry, GCD and EIS measurements were obtained with a BioLogic SP-150 potentiostat.

The EIS measurements of the SCs were carried out at DC bias of 100 mV over a frequency range from 100 mHz to 1 MHz.

The ionic conductivity of the gel type polyelectrolyte was obtained using the next formula:[10]

$$\sigma = \frac{L}{R_s \times A} \quad (1)$$

where the solution resistance (R_s) of the gel polyelectrolyte is obtained of the intercept of the real axis in the Nyquist plot, L is the separation between the electrodes and A is the area of the electrodes.

The areal capacitance of the SCs was obtained at two electrodes configuration by GCD technique was obtained with eqn (2).[18,21]

$$C = \frac{I\Delta t}{A\Delta t} \quad (2)$$

where I is the discharge current, Δt is the discharging time and A is the area of the electrode. The gravimetric capacitances were calculated in the same manner, but using the weight of the two electrodes instead of the area.

The energy (E) and power (P) densities were calculated by the following equations using the gravimetric capacitances:[18]

$$E = \frac{1}{2} C \Delta V^2 \quad (3)$$

$$P = \frac{E}{\Delta t} \quad (4)$$

Results and discussions

Polymer synthesis

The precursor polymers were obtained *via* metal-free, one-pot, super-acid catalyst polyhydroxyalkylation in a mixture with trifluoroacetic acid and methylenechloride at room temperature (Fig. 1). The polyhydroxyalkylation reaction has been widely used to obtain high molecular weight aromatic polymers without ether groups in the main chain that are susceptible to degradation.[22,23]

These features give these polymers high thermal, mechanical and chemical stability, which are desirable characteristics for applications in storage and energy conversion devices. The high solubility of the polymers allowed us to conduct NMR analysis to obtain the complete structural characterization. Proton NMR spectra show high regioselectivity in the polymerization reaction, and only *para* substitutions have been observed in the aromatic fragment.

Then, a polymer modification of the precursors was carried out through a substitution reaction with (3-bromopropyl)trimethylammonium bromide, affording the positively charged polyelectrolytes with different functionalization degrees (PNQA10, PNQA20, PNQA100 10, 20 and 100% functionalization degree respectively). The functionalization degree was determined by ^{1}H NMR (Fig. 2). The signals between 1.5 and 4.0 ppm correspond to the aliphatic protons belonging to (3-bromopropyl)trimethylammonium bromide.

This confirms the addition of the cationic group to the main chain, additionally, no other signal was observed above 9 ppm

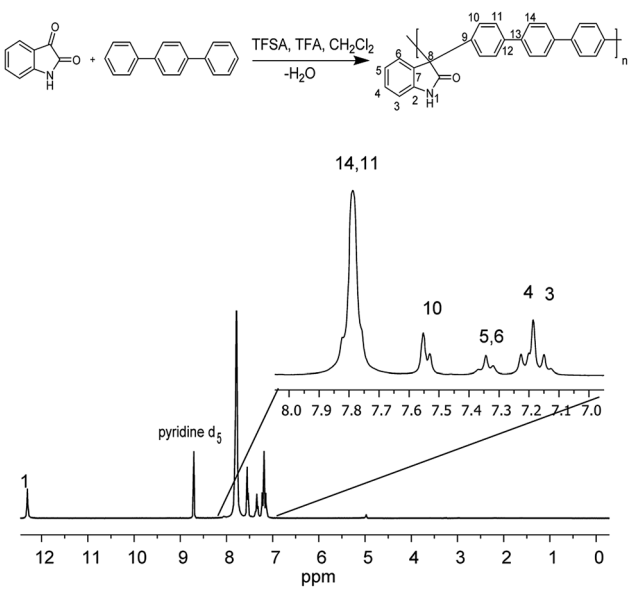

Fig. 1 Step polymerization of isatin with the nonactivated aromatic hydrocarbon *p*-terphenyl (top) and ^{1}H NMR spectra of precursor polymer (bottom).

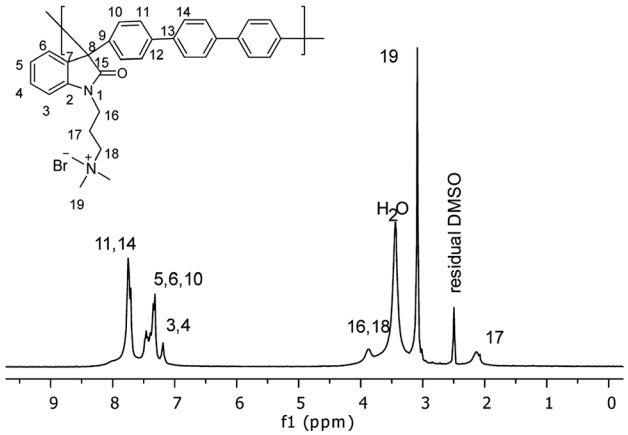

Fig. 2 ^{1}H NMR spectra of PNQA100 polyelectrolyte.

indicating the complete substitution of the precursor polymer with a 100% functionalization degree. In cases where lower degrees of functionalization were achieved, the observed signal around 9 ppm, corresponds to the amide proton associated with the isatin, corroborating the partial modification.[24] The organogel polyelectrolytes were obtained by dissolving the cationic fibbers 10% w/v in DMSO, the high molecular weight and phase segregation allow a three-dimensional arrangement tentatively due to the strong ionic interactions of the grafted fragment and the high hydrophobicity in the polymer backbone, leading to gelation processes without the need of chemical cross-linkers.

The supramolecular structures observed in this kind of polymers suggested self-assembled polymer structures[25] that are graphically represented in Fig. 3, allows different properties and are related to the degree of functionalization, we observed stronger supramolecular arrangements as the percentage of functionalization increases.

Ionic conductivity of the polyelectrolytes

The ionic conductivity of the different gel polymer electrolytes was measured by EIS to evaluate its potential use in SCs using eqn (1). The solution resistance (R_s) of the gel polyelectrolytes was obtained

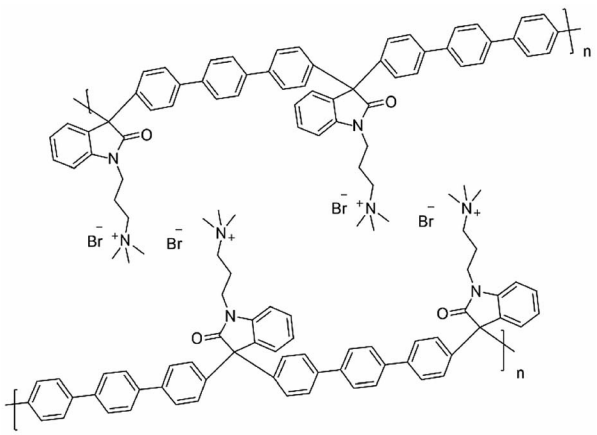

Fig. 3 Schematic model of supramolecular arrangement.

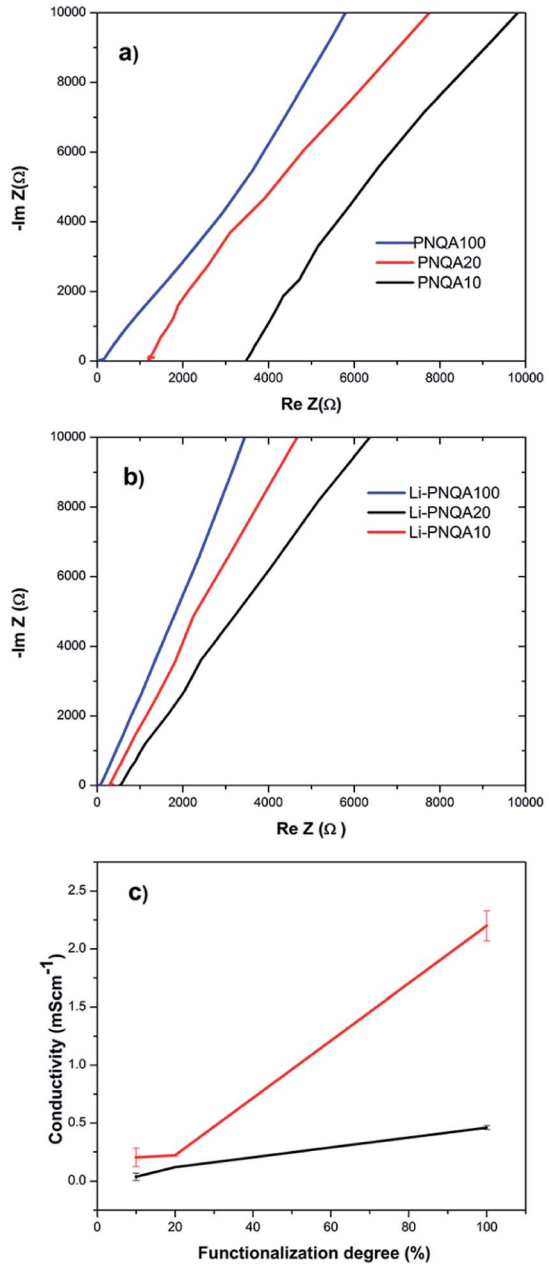

Fig. 4 (a) Nyquist plot of the PNQA10, PNQA20 and PNQA100 gel type polyelectrolytes, (b) Nyquist plot of the PNQA10, PNQA20 and PNQA100 gel type polyelectrolytes with 0.3 M lithium triflate (Li-PNQA10, Li-PNQA20 and Li-PNQA100) and (c) ionic conductivity of the organogel polyelectrolytes with (red line) and without (black line) lithium triflate with respect to the functionalization degree.

by the intersection of the real axis in the Nyquist plots[9] (Fig. 4a and b). The inclined line close to 90° in the low-frequency region confirms the capacitance behavior of the device.[10] The R_s of the gel polyelectrolyte decreases with the increment of the functionalization degree which is associated with an increase of positive charges in the polymer backbones. The solution resistance further decreases due to the addition of 0.3 M of lithium triflate due to the presence of extra ionic charges in the gel. Fig. 4c depicts the ionic conductivity with respect to the functionalization degree in the gel polyelectrolyte. The conductivity increases from 0.0362 to 0.118 mS cm^{-1} when the charged units increased from 10 (PNQA10) to 20% (PNQA20). After this functionalization degree, the ionic conductivity increases to 0.46 mS cm^{-1} for the 100% modified polymer (PNQA100).

The increase in conductivity with respect to the functionalization degree is probably due to a higher amount of ionic charges in the polymer. An increment of the ionic conductivity results suggests an increment of the double-layer capacitance for PNQA20 and PNQA100. The addition of a 0.3 M lithium triflate salt further increases the ionic conductivity at room temperature of the polyelectrolyte of the three different functionalization degrees. The polyelectrolytes with no salt addition show conductivities from 10^{-5} to 10^{-4} S cm^{-1} which are higher compared to that of insulating polymers, whose conductivities are in the order of 10^{-6} S cm^{-1} or lower. The doped polyelectrolytes with lithium triflate (Li-PNQA10, Li-PNQA20 and Li-PNQA100) showed a very similar behavior than the non-doped polyelectrolytes but with higher ionic conductivity.

The Li-PNQA20 (0.22 mS cm^{-1}) polymer presents a slightly increment with respect to Li-PNQA10 (0.2 mS cm^{-1}) meanwhile the Li-PNQA100 (2.26 mS cm^{-1}) display a considerable increment in comparison with the Li-doped polyelectrolytes with lower functionalization degree. In comparison with the polyelectrolytes without lithium triflate, there is an important increment of ionic conductivity with respect to the doped polyelectrolytes. These conductivities make this polyelectrolytes potential candidates to substitute the liquid electrolytes in SCs.

Capacitances of the SCs

The electrochemical properties and performance of the SCs were evaluated by cyclic voltammetry using a potential window of 0–

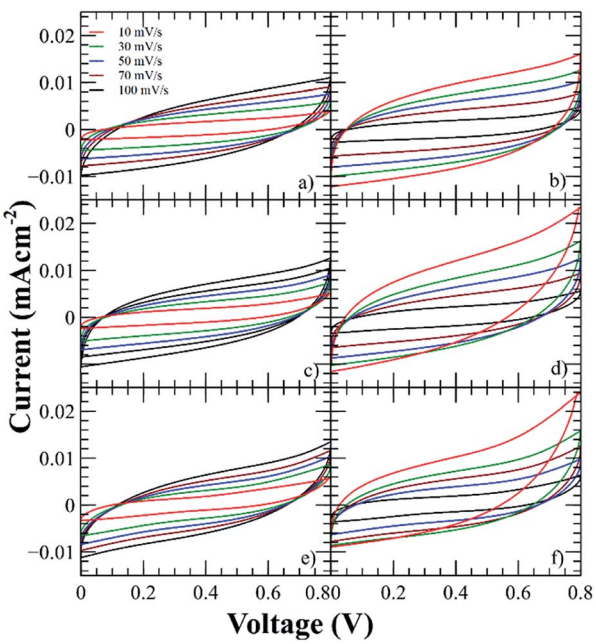

Fig. 5 Voltammograms of the SCs using the polyelectrolytes (a) PNQA10, (b) Li-PNQA10, (c) PNQA20, (d) Li-PNQA20, (e) PNQA100 and (f) Li-PNQA100.

0.8 V at different scan rates (from 10 to 100 mV s^{-1}). It can be observed in Fig. 5 that the CV curves present quasi-rectangular shape, therefore the SCs show an EDLC behavior.[8]

This EDLC is associated with an accumulation of electrostatic charge in the electrode–electrolyte interface due to an application of a potential between the electrodes.[26] While charging is taking place, the anions moves to the positive electrode and the cations, which are in the backbone, are orientated to the negative electrodes.[27] During discharge, the opposite processes occurred. Then, energy is storage in the double layer interfaces.

The current of the voltammograms showed an increment with respect to the functionalization degree, then the capacitance increases with respect to the charges in the polyelectrolyte due to the formation of a thicker EDLC and the addition of lithium triflate further increases the capacitances due to the addition of extra charges. The characteristic capacitive behavior was also examined by GCD technique at current densities in the range of 52 to 105 μA cm^{-2} (Fig. 6). The triangular shape of the curves with a very small IR drop demonstrates good rate capabilities.[9]

Using eqn (1), the areal capacitance was obtained for each functionalization degree with and without 0.3 M LiTf from the GCD curves. Fig. 7 displays the areal capacitances of the six different polyelectrolytes and shows that the capacitance is higher for lower scan rates due to the increase of the charge resistance of the polyelectrolyte.[9] The areal capacitances (gravimetric capacitances) obtained by GCD curves at 52 μA cm^{-2} of the PNQA10 polyelectrolyte is 0.68 mF cm^{-2} (18.85 mF g^{-1}) while at the same discharge current is 1.04 mF cm^{-2} (32.88 mF g^{-1}) for the SC using PNQA20. The SC with PNQA100 (1.17 mF cm^{-2}, 35.29 mF g^{-1}) shows an increment compared to the SC with the SCs using

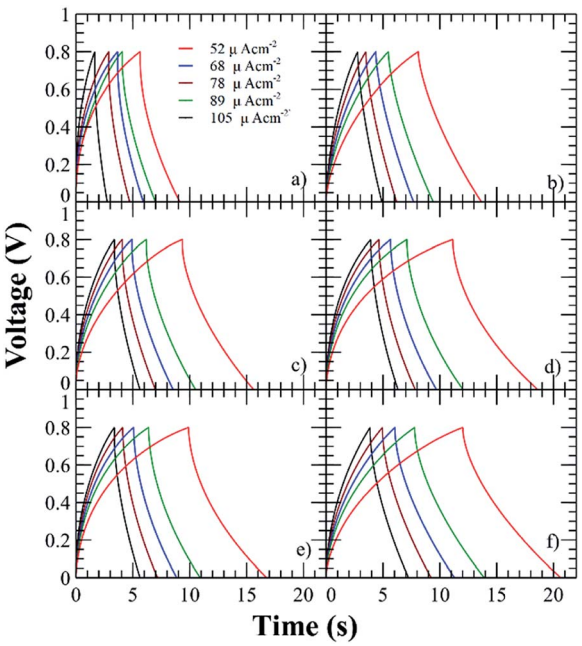

Fig. 6 GCD curves of the SCs using the polyelectrolytes (a) PNQA10, (b) Li-PNQA10, (c) PNQA20, (d) Li-PNQA20, (e) PNQA100 and (f) Li-PNQA100.

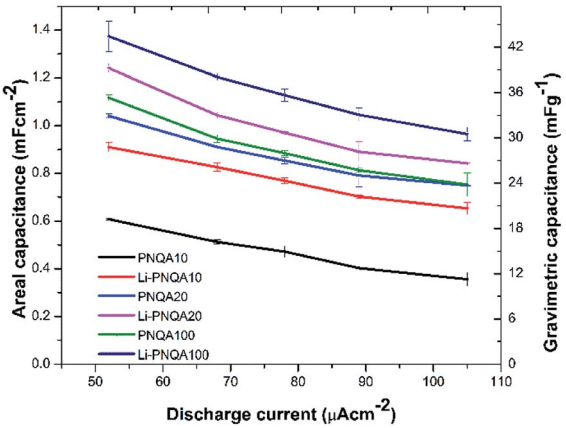

Fig. 7 Areal and gravimetric capacitances obtained by the GCD curves.

PNQA20 and PNQA10, which is consistent with the increase of ionic conductivity, therefore there is a correlation between ionic conductivity and capacitance. Doped polyelectrolytes with lithium triflate (Li-PNQA10, Li-PNQA20 and Li-PNQA100) display higher capacitances compared to the non-doped polyelectrolytes (areal capacitances of 0.909, 1.24 and 1.37 mF cm^{-2} and gravimetric capacitances of 28.74, 39.19 and 43.4 mF g^{-1}, for SC using Li-PNQA10, Li-PNQA20 and Li-PNQA100, respectively, at a discharge current of 52 μA cm^{-2}).

These capacitances are in the same order of magnitude compared to other gel polymer electrolytes with carbon nanotubes electrodes, activated carbon electrodes[7] or carbon nanotube fibber electrodes,[28] indicating that the cationic polymers with and without lithium triflate have potential application as polyelectrolytes and could represent an improvement of the capacitance using other electrodes like graphene, activated carbon or carbon nanotubes. At 52 μA cm^{-2} and using the eqn (3), the energy density of the SCs were calculated for PNQA10 (1.9 W h kg^{-1}), PNQA20 (3.04 W h kg^{-1}), and PNQA100 (3.16 W h kg^{-1}), respectively, meanwhile the Li-doped polyelectrolytes showed an increment of the energy density to 2.59, 3.48 and 3.8 W h kg^{-1} for Li-PNQA10, Li-PNQA20 and Li-PNQA, respectively. The power density of the SCs was calculated by eqn (4) and was 2280, 2202 and 1663 W kg^{-1} for the SCs with the undoped polyelectrolytes (PNQA10, PNQA20 and PNQA100, respectively) and 1365, 1581 and 1520 W kg^{-1} for the doped polyelectrolytes (Li-PNQA10, Li-PNQA20 and Li-PNQA100, respectively). These results of energy and power densities of this six polyelectrolytes are in the gap of the electrochemical capacitors or supercapacitors in the Ragone plot.[29]

Time stability of the SCs with the six polyelectrolytes was measured at a discharge current of 78 μA cm^{-2} for 1000 of charge–discharge cycles. Fig. S1† shows the 1st and 1000th charge–discharge cycles for each SC where it can be appreciated that the discharging time is decreasing due to the number of cycles. The Li-PNQA100 SC maintains the 65% of the initial capacitance, the PNQA100 SC the 50%, the Li-PNQA50 SC the 70.3%, the PNQA50 SC the 70%, the Li-PNQA20 SC the 81% and the PNQA20 the 50%.

This results obtained for energy and power densities of these SCs are in the same order as other SC using gel polyelectrolytes reported in the literature.[18,30]

Conclusions

In conclusion, polymer precursors were synthesized in a simple manner, the polyhydroxyalkylation reaction was performed in the Brønsted superacid trifluoromethanesulfonic acid (TFSA) and a mixture of TFSA with dichloromethane, the electrophilic aromatic substitutions reactions of isatin with *p*-terphenyl occurred exclusively in *para*-positions then a highly efficient post-polymerization functionalization was carried out to obtain cationic organogel polyelectrolytes. These results also suggest that a large variety of organogel polyelectrolytes could be obtained similarly. This work expands the scope of superelectrophilic polymerization and gel polyelectrolytes chemistries. These organogel polyelectrolytes were embedded between two commercial graphite electrodes to evaluate their performance in SCs. The cationic organogel polyelectrolytes showed an ionic conductivity in the order of $\sim 10^{-5}$ to 10^{-4} S cm^{-1} measured EIS depicting their potential application in energy storage devices. It was observed that the ionic conductivity increased as the percentage of charged monomers in the polymer backbone increases. The ionic conductivity further increased to the order of 10^{-3} S cm^{-1} (for Li-PNQA100) when a lithium salt was added. The areal capacitances of the SCs using these organogel polyelectrolytes were calculated by GCD and lie in the order of the mF cm^{-2} which is in agreement with other gel type polyelectrolytes reported in the literature. Additionally, the gravimetric capacitances are in the order of mF g^{-1}. It was found that the capacitances increased when the ionic conductivity increased due to the higher mobility of the charges in the polymer backbones, reaching these charges easily by the polyelectrolyte–electrode interface forming the electric double layer. The areal (gravimetric) capacitances of the SCs using the undoped polyelectrolytes was 0.68 mF cm^{-2} (18.85 mF g^{-1}), 1.04 mF cm^{-2} (32.88 mF g^{-1}) and 1.17 mF cm^{-2} (35.29 mF g^{-1}), for the SCs using PNQA10, PNQA20 and PNQA100 polyelectrolytes, respectively, measured at the same discharge current (52 μA cm^{-2}).

The Li-doped supercapacitors showed an increment of capacitance in comparison with the non-doped polyelectrolytes due to the presence of extra mobile charges, which causes a formation of a thicker double layer in the interfaces. The Li-PNQA100 SC showed the higher capacitance (1.37 mF cm^{-1}, 43.4 mF g^{-1}) at a discharging current of 52 μA cm^{-2} in comparison with the SC using Li-PNQA20 (1.24 mF cm^{-2}, 39.19 mF g^{-1}) and using Li-PNQA10 polyelectrolytes (0.9098 mF cm^{-2}, 28.74 mF g^{-1}) at the same discharge current.

The results presented in this work promise the possibility of modulating the capacitance in all solid-state SCs by chemical modifications and the use of thermal stable gel polyelectrolytes without the use of any dopant. Further research must be done to improve the electrochemical performance of the SC using carbon electrodes with a higher active area.

Conflicts of interest

There are no conflicts to declare.

Acknowledgements

The authors acknowledge the financial support from CONACYT Mexico Grant LANIAUTO 299092 and Ciencia Básica Grant A1-S-17967 and also for UC-MEXUS Grant CN-18-12. The technical support of Rebeca Leal, Abigail González and Miguel Flores is greatly appreciated. The authors gratefully acknowledge the help of Dr E. Coutino-González for proof-reading the document.

References

1 X. Cheng, J. Pan, Y. Zhao, M. Liao and H. Peng, *Adv. Energy Mater.*, 2017, **8**(7), 1702184.
2 D. P. Dubal, N. R. Chodankar, D. H. Kim and P. Gómez-Romero, *Chem. Soc. Rev.*, 2018, **47**, 2065–2129.
3 S. Palchoudhury, K. Ramasamy, R. K. Gupta and A. Gupta, *Front. Mater.*, 2019, **5**, 83.
4 X. Lu, M. Yu, G. Wang, Y. Tong and Y. Li, *Energy Environ. Sci.*, 2014, **7**, 2160–2181.
5 S. Chaudhari, Y. Sharma, P. S. Archana, R. Jose, S. Ramakrishna, S. Mhaisalkar and M. Srinivasan, *J. Appl. Polym. Sci.*, 2013, **129**(4), 1660–1668.
6 Poonam, K. Sharma, A. Arora and S. K. Tripathi, *J. Energy Storage*, 2019, **21**, 801–825.
7 Y. Kumar, G. P. Pandey and S. A. Hashmi, *J. Phys. Chem. C*, 2012, **116**(50), 26118–26127.
8 M. Moussa, M. F. El-Kady, Z. Zhao, P. Majewski and J. Ma, *Nanotechnology*, 2016, **27**(44), 442001.
9 W. G. Moon, G. P. Kim, M. Lee, H. D. Song and J. Yi, *ACS Appl. Mater. Interfaces*, 2015, **7**(6), 3503–3511.
10 H. Peng, B. Yao, X. Wei, T. Liu, T. Kou, P. Xiao, Y. Zhang and Y. Li, *Adv. Energy Mater.*, 2019, **9**(19), 1803665.
11 X. Peng, H. Liu, Q. Yin, J. Wu, P. Chen, G. Zhang, G. Liu, C. Wu and Y. Xie, *Nat. Commun.*, 2016, **7**, 11782.
12 H. Yu, J. Wu, L. Fan, Y. Lin, K. Xu, Z. Tang, C. Cheng, S. Tang, J. Lin, M. Huang and Z. Lan, *J. Power Sources*, 2012, **198**, 402–407.
13 J. Kötz, S. Kosmela and T. Beitz, Self-Assembled Polyelectrolyte Systems, *Prog. Polym. Sci.*, 2001, **26**(8), 1199–1232.
14 C. F. J. Faul and M. Antonietti, *Adv. Mater.*, 2003, **15**(9), 673–683.
15 L. Y. Liu, G. Xia, Z. J. Feng, Q. H. Hao and H. G. Tan, *Soft Matter*, 2019, **15**, 3689–3699.
16 C. F. J. Faul, *Acc. Chem. Res.*, 2014, **47**(12), 3428–3438.
17 Y. Huang, P. G. Lawrence and Y. Lapitsky, *Langmuir*, 2014, **30**, 7771–7777.
18 T. Cheng, Y. Z. Zhang, J. D. Zhang and W. L. W. Huang, *J. Mater. Chem. A*, 2016, **4**, 10493–10499.
19 H. Yu, J. Wu, L. Fan, K. Xu, X. Zhong, Y. Li and J. Lin, *Electrochim. Acta*, 2011, **56**(20), 6881–6886.

20 C. Zhu, P. Yang, D. Chao, X. Wang, X. Zhang, S. Chen, B. K. Tay, H. Huang, H. Zhang, W. Mai and H. J. Fan, *Adv. Mater.*, 2015, **27**(31), 4566–4571.
21 Y. Shao, M. F. El-Kady, C. W. Lin, G. Zhu, K. L. Marsh, J. Y. Hwang, Q. Zhang, Y. Li, H. Wang and R. B. Kaner, *Adv. Mater.*, 2016, **28**(31), 6719–6726.
22 L. I. Olvera, M. T. Guzmán-Gutiérrez, M. G. Zolotukhin, S. Fomine, J. Cárdenas, F. A. Ruiz-Treviño, D. Villers, T. A. Ezquerra and E. Prokhorov, *Macromolecules*, 2013, **46**(18), 7245–7256.
23 M. G. Zolotukhin, S. Fomine, R. Salcedo and L. Khalilov, *Chem. Commun.*, 2004, **8**, 1030–1031.
24 H. Hernández-Martínez, F. A. Ruiz-Treviño, J. Ortiz-Espinoza, M. J. Aguilar-Vega, M. G. Zolotukhin, R. Marcial-Hernandez and L. I. Olvera, *Ind. Eng. Chem. Res.*, 2018, **57**(13), 4640–4650.
25 W. H. Lee, E. J. Park, J. Han, D. W. Shin, Y. S. Kim and C. Bae, *ACS Macro Lett.*, 2017, **6**(5), 566–570.
26 G. Wang, L. Zhang and J. Zhang, *Chem. Soc. Rev.*, 2012, **41**, 797–828.
27 G. Wee, O. Larsson, M. Srinivasan, M. Berggren, X. Crispin and S. Mhalsalkar, *Adv. Funct. Mater.*, 2010, **20**, 4344–4350.
28 J. Ren, L. Li, C. Chen, X. Chen, Z. Cai, L. Qiu, Y. Wang, X. Zhu and H. Peng, *Adv. Mater.*, 2013, **25**, 1155–1159.
29 R. Kötz and M. Carlen, *Electrochim. Acta*, 2000, **45**, 2483–2498.
30 D. Ni, Y. Chen, H. Song, C. Liu, X. Yang and K. Cai, *J. Mater. Chem. A*, 2019, **7**, 1323–1333.